PHYSICAL REVIEW D **79,** 014003 (2009)

BCS-BEC crossover and phase structure of relativistic systems: A variational approach

Bhaswar Chatterjee*
Theory Division, Physical Research Laboratory, Navrangpura, Ahmedabad 380 009, India

Hiranmaya Mishra†
Theory Division, Physical Research Laboratory, Navrangpura, Ahmedabad 380 009, India
and School of Physical Sciences, Jawaharlal Nehru University, New Delhi-110067, India

Amruta Mishra‡
Department of Physics, Indian Institute of Technology, New Delhi-110016, India,
and Frankfurt Institute for Advanced Studies, Universität Frankfurt, D-60438 Frankfurt, Germany
(Received 8 April 2008; published 7 January 2009)

We investigate here the BCS-BEC crossover in relativistic systems using a variational construct for the ground state and the minimization of the thermodynamic potential. This is first studied in a four-fermion point interaction model and with a BCS type ansatz for the ground state with fermion pairs. It is shown that the antiparticle degrees of freedom play an important role in the BCS-BEC crossover physics, even when the ratio of Fermi momentum to the mass of the fermion is small. We also consider the phase structure for the case of fermion pairing with imbalanced populations. Within the ansatz, thermodynamically stable gapless modes for both fermions and antifermions are seen for strong coupling in the Bose-Einstein condensation (BEC) regime. We further investigate the effect of fluctuations of the condensate field by treating it as a dynamical field and generalize the BCS ansatz to include quanta of the condensate field also in a boson-fermion model with quartic self-interaction of the condensate field. It is seen that the critical temperature decreases with inclusion of fluctuations.

DOI: 10.1103/PhysRevD.79.014003 PACS numbers: 12.38.Mh, 24.85.+p

I. INTRODUCTION

Color superconductivity has become an active field of research during the last few years in the field of strong interaction physics [1]. At asymptotically high density the ground state of QCD is shown to be a color superconductor from first principle calculations [2]. However, for intermediate densities, relevant for the matter in the core of neutron stars, the perturbation theory breaks down and one uses effective models of strong interactions whose parameters are fitted to reproduce low energy hadronic properties. Although it is reassuring that certain quantities like the superconducting gap estimated from weak coupling QCD or using effective models like the Nambu-Jona-Lasinio (NJL) model yield similar magnitudes, the strong coupling dynamics at not so high densities remain uncontrolled. As the density decreases, before the quarks are confined, the coupling can become large enough so that the coherence length in the superconducting phase can be of the order of interparticle separation [3,4]. When this happens it is natural to imagine the quark-quark Cooper pairs as localized bound states rather than describing them as an extended macroscopic medium. At low enough temperature the ground state can then become a Bose-Einstein condensate (BEC) of diquark molecules. At still lower densities this diquark matter can undergo a confinement transition to form hadronic matter. The scenario that we have in mind is similar to as in Ref. [5], where, as the baryon density is increased, the baryonic matter undergoes a phase transition to a diquark BEC phase. The transition from BCS to BEC is most likely to be a crossover similar to their nonrelativistic counterparts in condensed matter systems like cold fermionic atoms. Various methods have been used recently to describe relativistic BCS-BEC crossover within a four-fermion point interaction model [4,6,7]. Effects of fluctuations have also been studied in the recent past to go beyond the mean field approximations [8–11] using a Gaussian approximation as well as including collective excitations [12]. Another interesting feature for the matter in the interior of neutron star is the variety of exotic non-BCS phases that arise when kinematical constraints (like neutrality) with respect to color and electric charges are imposed. Such stressed pairing has attracted attention both in quark matter [13] and in polarized Fermi gas of atoms [14,15]. Relativistic BCS-BEC crossover was also studied in a boson-fermion model and a rich phase structure was observed in such a system when there is a mismatch in the number densities of the condensing fermions [6].

Our approach to such problems in quark matter [16–18] as well as in cold atoms [19] has been variational. Charge

*bhaswar@prl.res.in
†hm@prl.res.in
‡amruta@physics.iitd.ac.in

neutral matter was considered with an explicit construct for the ground state in terms of quark pair operators as well as quark-antiquark operators. The ansatz functions in this construct were determined from the minimization of the thermodynamic potential subject to the constraints of neutrality conditions with respect to color and electrical charges. The effect of six-quark determinant interaction was also considered which highlighted the consequences of strange quark mass in such stressed pairing cases [20]. We apply here a similar method to study BCS-BEC crossover (as well as possible phase transition for mismatch in number densities) for a relativistic system in a fermionic theory with a four-Fermi point interaction model. As we shall demonstrate here the simple BCS type of ansatz for the ground state leads to results similar to the mean field results of a relativistic Bose-Fermi model [6]. This is demonstrated by taking a BCS type ansatz for the ground state and treating the condensate field as a classical auxiliary field. We next treat the condensate scalar field as a dynamical field and generalize the BCS ansatz to include the quanta of this condensate fields in a Bose-Fermi model with a quartic self-interaction for the scalar field. This improved ansatz for the ground state leads to a mass gap equation for the scalar field and the corresponding thermodynamic potential that can be obtained by resummation of bubble diagrams of perturbation theory similar to the results obtained in Cornwall-Jackiew-Tombolis (CJT) composite operator formalism [21,22].

We organize the paper as follows. In Sec. II we shall consider a relativistic model with a four-Fermi point interaction to discuss the BCS-BEC crossover physics. We shall take the bosonic condensate field as a classical auxiliary field while retaining the quantum nature of the fermionic field. In subsection II A, we spell out the ansatz for the ground state and in subsection II B, we evaluate the thermodynamic potential and consider the minimization of the same with respect to the ansatz functions. In Sec. III, we solve the gap equation and the number density equations and evaluate the thermodynamic potential. The thermodynamic potential for different phases is compared in this section to decide which phase is thermodynamically stable at what coupling and at what difference in the chemical potential. We also discuss our numerical results in this section. The results obtained in this section using the variational ansatz are similar to that obtained within mean field approximations in earlier calculations regarding BCS-BEC crossover and phase structure for imbalanced populations [4,6,7]. In Sec. IV, we treat the scalar condensate field as a dynamical field and generalize the ansatz of Sec. III to include the quanta of the fluctuations over and above the BCS ground state. We investigate this in a model with quartic self-interaction for the scalar field, calculating the mass of the scalar field self-consistently. We also include the effect of temperature in these calculations. Finally we summarize our results in Sec. V.

II. FERMIONIC MODEL FOR RELATIVISTIC SUPERFLUID

We shall consider a general relativistic model with only fermionic degrees of freedom in the Lagrangian. In particular we consider a general form for the Lagrangian given as

$$\mathcal{L} = \bar{\psi}^i(i\gamma^\mu\partial_\mu - m + \mu_i\gamma^0)\psi^i + \mathcal{L}_I \equiv \mathcal{L}_f + \mathcal{L}_I, \tag{1}$$

where ψ^i, $\bar{\psi}^i$ denote the Dirac fields with indices $i = 1, 2$ denoting the "flavor" for the fermions. Further, we have taken for simplicity both the fermions with the same mass m. With different masses, the Fermi energies or the chemical potential in the weak coupling can be different for the same number densities of the two pairing species. In the present analysis, for simplicity, we assume the masses of the pairing fermions to be the same, but consider their chemical potentials to be different.

To study superfluidity that results from Cooper pairing of two different flavors of fermions, we introduce the following local interaction term in the Lagrangian:

$$\mathcal{L}_I = -G(\bar{\psi}^i_c\gamma^5\psi^j|\epsilon^{ij}|)(\bar{\psi}^k\gamma^5\psi^l_c|\epsilon^{kl}|). \tag{2}$$

Here, G is the coupling constant, $\psi_c = C\bar{\psi}^T$, $\bar{\psi}_c = \psi^T C$, with the charge conjugation matrix being $C = i\gamma^2\gamma^0$. The $|\epsilon^{ij}|$ term ensures the cross flavor, spin zero antisymmetric pairing.

To illustrate the mean field calculation, introducing a field Φ, we can rewrite the interaction term as

$$\mathcal{L}_I = g|\epsilon^{ij}|(\bar{\psi}^i\gamma^5\psi^j_c\Phi + \bar{\psi}^i_c\gamma^5\psi^j\Phi^*) - m_b^2\Phi^*\Phi \tag{3}$$

with $G = g^2/m_b^2$ which can be identified upon elimination of the field Φ. We note that in the absence of a kinetic term the field Φ is an auxiliary field whose value in terms of the fermion bilinears is known. In the following, however, we shall treat the field Φ as a classical field and replace it by its expectation value while retaining the quantum nature for the fermion field. This will enable us to calculate the effective potential as a function of $\phi_0 = \langle\Phi\rangle$.

A. The ansatz for the ground state

To make the notations clear, let us first note that the fermion field operator expansion in momentum space is given as [23,24]

$$\begin{aligned}\psi(\mathbf{x}) &= \frac{1}{(2\pi)^{3/2}}\int \tilde{\psi}(\mathbf{k})e^{i\mathbf{k}\cdot\mathbf{x}}d\mathbf{k} \\ &= \frac{1}{(2\pi)^{3/2}}\int[U_0(\mathbf{k})q(\mathbf{k}) + V_0(-\mathbf{k})\tilde{q}(-\mathbf{k})]e^{i\mathbf{k}\cdot\mathbf{x}}d\mathbf{k},\end{aligned} \tag{4}$$

where

$$U_0(\mathbf{k}) = \begin{pmatrix} \cos(\frac{\chi^0}{2}) \\ \sigma \cdot \hat{k} \sin(\frac{\chi^0}{2}) \end{pmatrix},$$
$$V_0(-\mathbf{k}) = \begin{pmatrix} -\sigma \cdot \hat{k} \sin(\frac{\chi^0}{2}) \\ \cos(\frac{\chi^0}{2}) \end{pmatrix}. \quad (5)$$

The operators q and $\tilde{q}$ are the two component particle annihilation and antiparticle creation operators, respectively, which annihilate or create quanta acting upon the perturbative vacuum $|0\rangle$. We have suppressed here the flavor indices of the fermion field operators. The function $\chi^0(\mathbf{k})$ in the spinors in Eq. (5) are given as $\cot\chi_i^0 = m_i/|\mathbf{k}|$, for free massive fermion fields, i being the flavor index. For massless fields $\chi^0(|\mathbf{k}|) = \pi/2$. We shall in the following however consider for simplicity $m_1 = m_2 = m$. We shall use the notations and conventions of Ref. [17,18] and recapitulate briefly the construction of the variational ansatz for the ground state. We take it as a squeezed coherent state with fermion condensates given as [16–18]

$$|\Omega\rangle = \mathcal{U}_d|0\rangle. \quad (6)$$

Here, $\mathcal{U}_d$ is a unitary operator which creates fermion pairs. Explicitly, the operator $\mathcal{U}_d$ is given as

$$\mathcal{U}_d = \exp(B_d^\dagger - B_d), \quad (7)$$

where $B_d^\dagger$ is the pair creation operator as given by

$$B_d^\dagger = \int [q_r^i(\mathbf{k})^\dagger r f(\mathbf{k}) q_{-r}^j(-\mathbf{k})^\dagger |\epsilon_{ij}|] d\mathbf{k} + \int [\tilde{q}_r^i(\mathbf{k}) r f_1(\mathbf{k}) \tilde{q}_{-r}^j(-\mathbf{k}) |\epsilon_{ij}|] d\mathbf{k}. \quad (8)$$

In the above, i, j are flavor indices, and $r(= \pm 1/2)$ is the spin index. Further, $f(\mathbf{k})$ and $f_1(\mathbf{k})$ are ansatz functions associated with fermion pairs and antifermion pairs describing the condensates and shall be determined by the minimization of the thermodynamic potential. Note that we have assumed these "condensate functions" $f(\mathbf{k})$ and $f_1(\mathbf{k})$ to be independent of flavor indices. We give a *post-facto* justification for this to be that the functions depend upon the *average* energy and *average* chemical potential of the fermions/antifermions that condense.

Finally, to include the effects of temperature and density we write down the state at finite temperature and density $|\Omega(\beta, \mu)\rangle$ taking a thermal Bogoliubov transformation over the state $|\Omega\rangle$ using thermo field dynamics (TFD) as described in Refs. [25,26]. We then have

$$|\Omega(\beta, \mu)\rangle = \mathcal{U}_{\beta,\mu}|\Omega\rangle = \mathcal{U}_{\beta,\mu}\mathcal{U}_d|0\rangle, \quad (9)$$

where $\mathcal{U}_{\beta,\mu}$ is given as

$$\mathcal{U}_{\beta,\mu} = e^{\mathcal{B}^\dagger(\beta,\mu) - \mathcal{B}(\beta,\mu)}, \quad (10)$$

with

$$\mathcal{B}^\dagger(\beta, \mu) = \int [q'(\mathbf{k})^\dagger \theta_-(\mathbf{k}, \beta, \mu) \underline{q}'(\mathbf{k})^\dagger] d\mathbf{k} + \int [\tilde{q}'(\mathbf{k}) \theta_+(\mathbf{k}, \beta, \mu) \tilde{q}'(\mathbf{k})] d\mathbf{k}. \quad (11)$$

In Eq. (11) the ansatz functions $\theta_\pm(\mathbf{k}, \beta, \mu)$ will be related to quark and antiquark distributions and the underlined operators are the operators in the extended Hilbert space associated with thermal doubling in the TFD method. In Eq. (11) we have suppressed the flavor indices in the fermion operators as well as in the functions $\theta(\mathbf{k}, \beta, \mu)$.

All the functions in the ansatz in Eq. (9) are to be obtained by minimizing the thermodynamic potential. We shall carry out this minimization in the next subsection.

B. Evaluation of thermodynamic potential and gap equations

To calculate the thermodynamic potential corresponding to the Lagrangian of Eq. (1) and (3) and the state given in Eq. (9), we first write down the expectation values of the following fermion operator bilinears:

$$\langle\Omega(\beta, \mu)|\tilde{\psi}_\gamma^i(\mathbf{k})\tilde{\psi}_\delta^j(\mathbf{k}')^\dagger|\Omega(\beta, \mu)\rangle = \delta^{ij}\Lambda^i_{+\gamma\delta}(\mathbf{k}, \beta, \mu)\delta(\mathbf{k} - \mathbf{k}') \quad (12)$$

and

$$\langle\Omega(\beta, \mu)|\tilde{\psi}_\delta^{i\dagger}(\mathbf{k})\tilde{\psi}_\gamma^j(\mathbf{k}')|\Omega(\beta, \mu)\rangle = \delta^{ij}\Lambda^i_{-\gamma\delta}(\mathbf{k}, \beta, \mu)\delta(\mathbf{k} - \mathbf{k}'), \quad (13)$$

where

$$\Lambda^i_{\pm\gamma\delta}(\mathbf{k}, \beta, \mu) = \frac{1}{2}[1 \pm (F_1^i(\mathbf{k}) - F^i(\mathbf{k})) \pm (\gamma^0 \cos\chi^i(\mathbf{k}) + \boldsymbol{\alpha} \cdot \hat{\mathbf{k}} \sin\chi^i(\mathbf{k})) \times (1 - F^i(\mathbf{k}) - F_1^i(\mathbf{k}))]_{\gamma\delta}. \quad (14)$$

In the above, $\tilde{\psi}(\mathbf{k})$ is the Fourier transform of $\psi(\mathbf{x})$ [18]. The effect of the fermion condensates and their temperature and/or density dependences are encoded in the functions $F^i(\mathbf{k})$ and $F_1^i(\mathbf{k})$ given as

$$F^i(\mathbf{k}) = (\sin^2\theta^i_-(\mathbf{k}) + \sin^2 f(\mathbf{k}) \cos 2\theta^{i,j}_-(\mathbf{k})) \quad (15)$$

and

$$F_1^i(\mathbf{k}) = (\sin^2\theta^i_+(\mathbf{k}) + \sin^2 f_1(\mathbf{k}) \cos 2\theta^{i,j}_+(\mathbf{k})). \quad (16)$$

We have defined $\cos 2\theta^{i,j}_\pm = 1 - \sin^2\theta^i_\pm - \sin^2\theta^j_\pm$ with $i \neq j$.

For difermion operators, we have

$$\langle\Omega(\beta, \mu)|\psi_\alpha^i(\mathbf{x})\psi_\gamma^j(\mathbf{0})|\Omega(\beta, \mu)\rangle = -\frac{1}{(2\pi)^3}\int e^{i\mathbf{k}\cdot\mathbf{x}}\mathcal{P}^{i,j}_{+\gamma\alpha}(\mathbf{k}, \beta, \mu)d\mathbf{k} \quad (17)$$

and

$$\langle\Omega(\beta,\mu)|\psi^{i\dagger}_{\alpha}(\mathbf{x})\psi^{j\dagger}_{\gamma}(\mathbf{0})|\Omega(\beta,\mu)\rangle = -\frac{1}{(2\pi)^3}\int e^{i\mathbf{k}\cdot\mathbf{x}}\mathcal{P}^{i,j}_{-\alpha\gamma}(\mathbf{k},\beta,\mu)d\mathbf{k}, \tag{18}$$

where

$$\mathcal{P}^{i,j}_{+}(\mathbf{k},\beta,\mu) = \frac{|\epsilon^{ij}|}{4}\Big[S^{i,j}(\mathbf{k})\Big(\cos\Big(\frac{\chi_i-\chi_j}{2}\Big) - \boldsymbol{\gamma}\cdot\hat{\mathbf{k}}\sin\Big(\frac{\chi_i-\chi_j}{2}\Big)\Big) + \Big(\gamma^0\cos\Big(\frac{\chi_i+\chi_j}{2}\Big) - \boldsymbol{\alpha}\cdot\hat{\mathbf{k}}\sin\Big(\frac{\chi_i+\chi_j}{2}\Big)\Big)A^{i,j}(\mathbf{k})\Big]\gamma_5 C \tag{19}$$

$$\mathcal{P}^{i,j}_{-}(\mathbf{k},\beta,\mu) = \frac{|\epsilon^{ij}|C\gamma_5}{4}\Big[S^{i,j}(\mathbf{k})\Big(\cos\Big(\frac{\chi_i-\chi_j}{2}\Big) + \boldsymbol{\gamma}\cdot\hat{\mathbf{k}}\sin\Big(\frac{\chi_i-\chi_j}{2}\Big)\Big) + \Big(\gamma^0\cos\Big(\frac{\chi_i+\chi_j}{2}\Big) - \boldsymbol{\alpha}\cdot\hat{\mathbf{k}}\sin\Big(\frac{\chi_i+\chi_j}{2}\Big)\Big)A^{i,j}(\mathbf{k})\Big]. \tag{20}$$

Here, $C = i\gamma^2\gamma^0$ is the charge conjugation matrix (we use the notation of Bjorken and Drell) and the functions $S(\mathbf{k})$ and $A(\mathbf{k})$ are given as

$$S^{i,j}(\mathbf{k}) = \sin 2f(\mathbf{k})\cos 2\theta^{i,j}_{-}(\mathbf{k},\beta,\mu) + \sin 2f_1(\mathbf{k})\cos 2\theta^{i,j}_{+}(\mathbf{k},\beta,\mu), \tag{21}$$

and

$$A^{i,j}(\mathbf{k}) = \sin 2f(\mathbf{k})\cos 2\theta^{i,j}_{-}(\mathbf{k},\beta,\mu) - \sin 2f_1(\mathbf{k})\cos 2\theta^{i,j}_{+}(\mathbf{k},\beta,\mu). \tag{22}$$

These expressions are used to calculate the thermal expectation value of the Hamiltonian and to compute the thermodynamic potential given as

$$\Omega = \epsilon - \mu^i\rho^i - \frac{1}{\beta}s, \tag{23}$$

where ϵ is the energy density and s is the entropy density and $\rho^i = \langle\psi^{i\dagger}\psi^i\rangle$ $(i = 1, 2)$ is the number density of i-th species.

It is then straightforward to calculate the expectation value of the Hamiltonian corresponding to the Lagrangian given in Eq. (1) and (3). This can be written as

$$\epsilon - \mu^i\rho^i = \langle H - \mu^i\psi^{i\dagger}\psi^i\rangle = T + V_D. \tag{24}$$

Explicitly, the kinetic energy minus the $\mu^i\rho^i$ part is given as

$$T \equiv \langle\Omega(\beta,\mu)|\psi^{\dagger}_i(-i\boldsymbol{\alpha}\cdot\boldsymbol{\nabla} + \gamma^0 m - \mu^i)\psi_i|\Omega(\beta,\mu)\rangle = \frac{2}{(2\pi)^3}\sum_{i=1}^{2}\int d\mathbf{k}(\sqrt{\mathbf{k}^2+m^2}(F^i + F^i_1) - \mu^i(F^i - F^i_1)), \tag{25}$$

where F^i and F^i_1 are given by Eqs. (15) and (16). Here we have subtracted out the vacuum contributions.

Similarly, the contribution from the interaction from Eq. (3) to the energy density is given as

$$V_D = -\langle\Omega(\beta,\mu)|\mathcal{L}_I|\Omega(\beta,\mu)\rangle = -4gI_D\phi_0 + m_b^2\phi_0^2, \tag{26}$$

where we have taken ϕ_0 to be real. In the above,

$$I_D = \frac{1}{2}\langle\bar{\psi}^i_c\gamma^5|\epsilon^{ij}|\psi^j\rangle = \frac{1}{(2\pi)^3}\int d\mathbf{k}[\sin 2f(\mathbf{k})(1 - \sin^2\theta^1_- - \sin^2\theta^2_-) + \sin 2f_1(\mathbf{k})(1 - \sin^2\theta^1_+ - \sin^2\theta^2_+)] \tag{27}$$

which is proportional to the fermion condensate.

Finally, to calculate the thermodynamic potential we have to include the entropy density for the fermions. This is given as [25]

$$s = -\frac{2}{(2\pi)^3}\sum_i\int d\mathbf{k}(\sin^2\theta^i_-\,\mathrm{lnsin}^2\theta^i_- + \cos^2\theta^i_-\,\mathrm{lncos}^2\theta^i_- + \sin^2\theta^i_+\,\mathrm{lnsin}^2\theta^i_+ + \cos^2\theta^i_+\,\mathrm{lncos}^2\theta^i_+). \tag{28}$$

The extremization of the thermodynamic potential Eq. (23) with respect to the condensate functions $f(\mathbf{k})$ and $f_1(\mathbf{k})$ yields

$$\tan 2f(\mathbf{k}) = \frac{2g\phi_0}{\bar{\epsilon}-\bar{\mu}} \equiv \frac{\Delta}{\bar{\epsilon}-\bar{\mu}} \tag{29}$$

and

$$\tan 2f_1(\mathbf{k}) = \frac{2g\phi_0}{\bar{\epsilon}+\bar{\mu}} \equiv \frac{\Delta}{\bar{\epsilon}+\bar{\mu}}, \tag{30}$$

where we have defined the superconducting gap $\Delta = 2g\phi_0$. In the above $\bar{\epsilon} = (\epsilon_1+\epsilon_2)/2$ and $\bar{\mu} = (\mu_1+\mu_2)/2$ with $\epsilon_i = \sqrt{\mathbf{k}^2+m_i^2}$. It is thus seen that the condensate functions depend upon the *average* energy and the *average* chemical potential of the fermions/antifermions that condense.

Finally, the minimization of the thermodynamic potential with respect to the thermal functions $\theta_{\pm}(\mathbf{k})$ gives

$$\sin^2\theta^i_{\pm}(\mathbf{k}) = \frac{1}{\exp(\beta\omega^{(i)}_{\pm})+1}, \tag{31}$$

where

$$\omega_{\pm}^{(1)} = \bar{\omega}_{\pm} + \delta_{\epsilon} \pm \delta_{\mu} \tag{32}$$

and

$$\omega_{\pm}^{(2)} = \bar{\omega}_{\pm} - \delta_{\epsilon} \mp \delta_{\mu}. \tag{33}$$

Here, $\bar{\omega}_{\pm} = \sqrt{\Delta^2 + \bar{\xi}_{\pm}^2}$, $\bar{\xi}_{\pm} = (\xi_{1\pm} + \xi_{2\pm})/2$, $\xi_{i\pm} = \epsilon_i \pm \mu_i$. Further, the chemical potential difference $\delta_{\mu} = (\mu_1 - \mu_2)/2$ and $\delta_{\epsilon} = (\epsilon_1 - \epsilon_2)/2$. Notice that for $\delta_{\mu} > 0$ and for equal masses for the two species $\delta_{\epsilon} = 0$ with $\epsilon_1 = \epsilon_2 = \epsilon = \sqrt{\mathbf{k}^2 + m^2}$, we can have the possibility of gapless modes for $\omega_{-}^{(1)}$ or $\omega_{+}^{(2)}$.

Using these dispersion relations, and substituting the condensate functions and the distribution functions, leads to the thermodynamics potential given by Eq. (23), as

$$\begin{aligned}\Omega = &\frac{2}{(2\pi)^3}\int(2\epsilon - \bar{\omega}_- - \bar{\omega}_+)d\mathbf{k} \\ &- \frac{2}{(2\pi)^3\beta}\sum_i \int d\mathbf{k}[\ln(1 + e^{(-\beta\omega_-^{(i)})}) \\ &+ \ln(1 + e^{(-\beta\omega_+^{(i)})})] + m_b^2\phi_0^2.\end{aligned} \tag{34}$$

Here the extremization over ϕ_0 is yet to be done. An extremization with respect to ϕ_0 leads to the gap equation

$$\frac{m_b^2}{4g^2} = \int \frac{d\mathbf{k}}{(2\pi)^3}\left[\frac{\cos 2\theta_-^{1,2}}{\bar{\omega}_-} + \frac{\cos 2\theta_+^{1,2}}{\bar{\omega}_+}\right], \tag{35}$$

with $\cos 2\theta_{\mp}^{1,2} = 1 - \sin^2\theta_{\mp}^1 - \sin^2\theta_{\mp}^2$.

The gap equation is quadratically divergent which is rendered finite in the NJL model with a momentum cutoff Λ. In the nonrelativistic case this is rendered finite by subtracting out the vacuum contribution and relating the four-fermion coupling to the s-wave scattering length [19,27]. A similar approach can be done for the relativistic case also by relating the coupling to the s-wave scattering length. This leads to the renormalized gap equation [7]

$$\begin{aligned}-\frac{m}{4\pi a} = \int \frac{d\mathbf{k}}{(2\pi)^3}\Bigg[&\frac{\cos 2\theta_-^{1,2}}{\bar{\omega}_-} + \frac{\cos 2\theta_+^{1,2}}{\bar{\omega}_+} - \frac{1}{\epsilon - m} \\ &- \frac{1}{\epsilon + m}\Bigg].\end{aligned} \tag{36}$$

However, after this subtraction, unlike the nonrelativistic case, the ultraviolet cutoff dependence is still there in the above gap equation, although the dependence is milder. We might also note that one could have defined a renormalized boson mass $m_{b,r}$ with $m_{b,r}^2 = \partial\Omega/\partial\phi_0^2|_{\phi_0=T=0,\mu=m}$ as in Ref. [6] and one would have arrived at the same gap equation. For the present, we shall take the renormalized coupling as in Eq. (36) and treat this as the crossover parameter. As a function of this coupling one has to calculate the gap parameter Δ for different densities of the fermions of the two species. The average number density is given as

$$\bar{\rho} = \frac{\rho_1 + \rho_2}{2} = \rho_- - \rho_+, \tag{37}$$

where the fermionic component is given as

$$\rho_- = -\frac{1}{(2\pi)^3}\int \frac{\bar{\xi}_-}{\bar{\omega}_-}\cos 2\theta_-^{1,2} d\mathbf{k} \tag{38}$$

and the antifermionic component of the average number density is

$$\rho_+ = -\frac{1}{(2\pi)^3}\int \frac{\bar{\xi}_+}{\bar{\omega}_+}\cos 2\theta_+^{1,2} d\mathbf{k}, \tag{39}$$

where $\cos 2\theta_{\mp}^{1,2} = (1 - \sin^2\theta_{\mp}^1(\mathbf{k}) - \sin^2\theta_{\mp}^2(\mathbf{k}))$ with $\sin^2\theta_{\pm}^i(\mathbf{k})$ being the thermal distribution functions for the fermions defined in Eq. (31). The difference in the number densities is given as

$$\begin{aligned}\delta_{\rho} &= \frac{\rho_1 - \rho_2}{2} \\ &= \frac{1}{(2\pi)^3}\int[(\sin^2\theta_-^1 - \sin^2\theta_+^1) \\ &\quad - (\sin^2\theta_-^2 - \sin^2\theta_+^2)]d\mathbf{k},\end{aligned} \tag{40}$$

$\rho^i = \langle\psi^{i\dagger}\psi^i\rangle$, where the expectation value is taken with respect to the state given in Eq. (9).

Using the gap equation (35), the thermodynamic potential given by Eq. (34) can be rewritten as

$$\begin{aligned}\Omega(\Delta, \bar{\mu}, \delta_{\mu}, \beta) = \frac{2}{(2\pi)^3\beta}\int d\mathbf{k}\Bigg[&\Bigg(\bar{\xi}_- - \bar{\omega}_- + \frac{\Delta^2}{2\bar{\omega}_-} \\ &+ \bar{\xi}_+ - \bar{\omega}_+ + \frac{\Delta^2}{2\bar{\omega}_+}\Bigg) \\ &- \sum_i\{\ln(1 + e^{(-\beta\omega_-^{(i)})}) \\ &+ \ln(1 + e^{(-\beta\omega_+^{(i)})})\}\Bigg].\end{aligned} \tag{41}$$

To compare the stability of various phases we compare the thermodynamic potentials of these phases with respect to that of normal matter. This can be obtained from Eq. (41) in the limit of gap $\Delta \to 0$. We consider the difference in the thermodynamic potentials between condensed phase and the normal matter as given by

$$\tilde{\Omega}(\Delta, \bar{\mu}, \delta_\mu, \beta) = \Omega(\Delta, \bar{\mu}, \delta_\mu, \beta) - \Omega(\Delta = 0, \bar{\mu}, \delta_\mu, \beta)$$
$$= \frac{2}{(2\pi)^3}\int\left(|\bar{\xi}_-| - \bar{\omega}_- + \frac{\Delta^2}{2\bar{\omega}_-}\cos 2\theta_-^{1,2} + |\bar{\xi}_+| - \bar{\omega}_+ + \frac{\Delta^2}{2\bar{\omega}_+}\cos 2\theta_+^{1,2}\right)d\mathbf{k}$$
$$- \frac{2}{(2\pi)^3\beta}\sum_{i=1,2}\int[\{\ln(1 + e^{(-\beta\omega_-^{(i)})}) + \ln(1 + e^{(-\beta\omega_+^{(i)})})\} - \{\ln(1 + e^{(-\beta\omega_{0-}^{(i)})} - \ln(1 + e^{(-\beta\omega_{0+}^{(i)})})\}]d\mathbf{k}. \tag{42}$$

In the above, $\omega_{0\mp}^{(1)} = |\bar{\xi}_\mp| \mp \delta_\mu$, $\omega_{0\mp}^{(2)} = |\bar{\xi}_\mp| \pm \delta_\mu$ correspond to the normal matter dispersion relations for the two species. For stability of the condensed phase, $\tilde{\Omega}$ has to be negative with Δ and $\bar{\mu}$ determined from the gap equation (36) and the number density equation (37). Further, one has to ensure that the solution corresponds to a minimum and not a maximum. In what follows we shall restrict ourselves to the case of zero temperature only. As noted earlier we shall consider here without loss of generality $\delta_\mu > 0$. Also we consider a system of equal masses for the fermions so that $\delta_\epsilon = 0$. This leads to the possibility of quasiparticle energy for species 1, $\omega^{(1)}$ or the quasiantifermion energy for species 2, $\omega_+^{(2)}$ becoming negative. In that case the distribution functions given by Eq. (31) become Heaviside (Θ) functions i.e. $\sin^2\theta^a = \Theta(-\omega_a)$. Further, using the identity $\lim_{a\to\infty}\ln(1 + \exp(-ax))/a = -x\Theta(-x)$ in Eq. (42), the zero temperature thermodynamic potential becomes

$$\tilde{\Omega}_0(\Delta, \bar{\mu}, \delta_\mu) = \frac{2}{(2\pi)^3}\int\left(|\bar{\xi}_-| - \bar{\omega}_- + \frac{\Delta^2}{2\bar{\omega}_-} + |\bar{\xi}_+| - \bar{\omega}_+ + \frac{\Delta^2}{2\bar{\omega}_+}\right)d\mathbf{k}$$
$$+ \frac{2}{(2\pi)^3}\int\left[\left(\omega_-^{(1)} - \frac{\Delta^2}{2\bar{\omega}_-}\right)\theta(-\omega_-^{(1)}) + \left(\omega_+^{(2)} - \frac{\Delta^2}{2\bar{\omega}_+}\right)\theta(-\omega_+^{(2)}) - \omega_{0-}^{(1)}\theta(-\omega_{0-}^{(1)}) - \omega_{0+}^{(2)}\theta(-\omega_{0+}^{(2)})\right]d\mathbf{k}. \tag{43}$$

Equations (36) and (37) need to be solved self-consistently to determine the gap as a function of the coupling and its stability will be decided by calculating the thermodynamic potential. We note here that BEC is usually discussed using the canonical ensemble where the particle number density is fixed as an external parameter. We shall also consider fixed number density here to discuss BCS-BEC crossover/phase transition in the relativistic fermionic system [6,8–11]. However, we might also note here that, to discuss quark matter, one usually employs the grand canonical ensemble with a fixed quark chemical potential to explore the QCD phase diagram in the chemical potential and temperature plane. In the numerical calculation that follows we keep the average number density fixed and consider the solutions as a function of the coupling and the difference in chemical potentials. Sometimes we find multiple solutions for the gap and average chemical potential satisfying Eqs. (36) and (37) corresponding to multiple extrema of the thermodynamic potential. In such cases, the solution which has the least thermodynamic potential is chosen. We also verify the positivity for the second derivative of the thermodynamic potential for this solution. This way we ensure that the pair of solutions for superfluid gap and the chemical potential corresponds to the minimum of the thermodynamic potential. The detailed numerical calculations of the present investigation are discussed in the next section.

III. NUMERICAL SOLUTION OF THE GAP EQUATION AND PHASE STRUCTURE

For numerical calculations it is convenient to introduce the dimensionless quantities in terms of Fermi momentum k_f or Fermi energy $\epsilon_f = \sqrt{k_f^2 + m^2}$, defined through $|\mathbf{k}| = k_f x$, $\eta = 1/(k_f a)$, $m = k_f\hat{m}$, $\Delta = \epsilon_f z$, $\mu = \epsilon_f\hat{\mu}$. The gap equation at zero temperature can then be written as

$$-\frac{\eta}{2} = \frac{1}{\hat{m}\pi}\int_0^{x_{\max}} dx x^2\left(\frac{1}{\hat{\omega}_-} + \frac{1}{\hat{\omega}_+} - \frac{2\epsilon(x)}{x^2}\right.$$
$$\left. - \frac{1}{\hat{\omega}_-^{(1)}}\Theta(-\hat{\omega}_-^{(1)}) - \frac{1}{\hat{\omega}_-^{(2)}}\Theta(-\hat{\omega}_-^{(2)})\right). \tag{44}$$

Similarly, the equation for the average number density given by Eq. (37) can be rewritten in terms of these dimensionless quantities as

$$1 = 1.5\int_0^{x\max} dx x^2\left[\frac{\hat{\xi}_+(x)}{\hat{\omega}_+(x)}(1 - \Theta(-\hat{\omega}_+^{(2)}))\right.$$
$$\left. - \frac{\hat{\xi}_-(x)}{\hat{\omega}_-(x)}(1 - \Theta(-\hat{\omega}_-^{(1)}))\right] \tag{45}$$

for the average density. Here, $\hat{\xi}_\pm(x) = \hat{\epsilon}(x) \pm \hat{\mu}\sqrt{(1 + \hat{m}^2)}$, $\hat{\epsilon}(x) = \sqrt{x^2 + \hat{m}^2}$, $\hat{\omega}_\pm = \sqrt{\hat{\xi}_\pm^2 + z^2(1 + \hat{m}^2)}$,

and finally $x_{\max} = \Lambda/k_f$ is the upper cutoff for momentum in units of Fermi momentum κ_f. Here $\tilde{\bar{\mu}}$ is the average of the chemical potentials of the two species in units of Fermi energy.

To analyze the crossover, let us first consider the symmetric case—namely when the chemical potential difference between the two species is zero. In this limit, $\Theta(-\omega^{(i)}_{\pm})$ become zero in both Eqs. (44) and (45). We note that we have essentially three-dimensional quantities in the problem: the cutoff Λ, the mass of the fermion m, and the scattering length a. We further note that the dimensional coupling G is bounded above with a critical value $G_c\Lambda^2 > 2\pi^2$, beyond which the zero density vacuum itself is unstable to form fermion pairs leading to a Majorana mass for the fermions.

We might note here that at zero density, the minimum excitation energy for the fermion is its mass m. For a normal matter, with a finite chemical potential it is $(m - \mu)$. In the BEC state, the decay mode of the bound state is that of the bound state going to two fermions. The threshold for this energy is thus $2(m - \mu)$. The bosonic bound state should therefore be stable if this threshold energy is positive, which in turn means that $m > \mu$. This we shall take as our working definition for BEC phase to distinguish between the BCS and BEC phase as we increase the dimensionless coupling parameter η from weak coupling BCS (large negative η) to strong coupling BEC phase (large positive η) through unitary limit ($\eta = 0$).

For numerical calculations, we choose the parameters $x_{\max} = \Lambda/k_f = 50$, $\hat{m} = m/k_f = 5$, and study the results by varying the dimensionless coupling η from negative to positive values. The resulting gap parameter and the chemical potential are plotted in Figs. 1 and 2. To show the contribution of the antiparticle degrees of freedom we have plotted the results obtained by solving the coupled gap equations (44) and (45), without and with the antiparticle contributions.

One might naively expect that for this nonrelativistic $k_f/m = 0.2$ case, the antiparticle channel is suppressed. But as may be seen from Fig. 1, while such an expectation may be the situation for the weak coupling BCS regime, these contributions become increasingly important as the coupling increases. As the coupling increases, the chemical potential $\tilde{\mu} = \mu - m$ decreases and changes sign at coupling $\eta \approx 1.04$ signaling the BEC regime. To appreciate the relativistic effects we also consider the case with $m/k_f = 0.67$ and $\Lambda/k_f = 3.3$ [6] and the resulting gap and the chemical potential are shown in Fig. 3.

As we might observe, in the weak coupling BCS limit (large negative η), the chemical potential is given by the Fermi energy. With increase in the coupling, the chemical potential decreases and becomes negligible as compared to

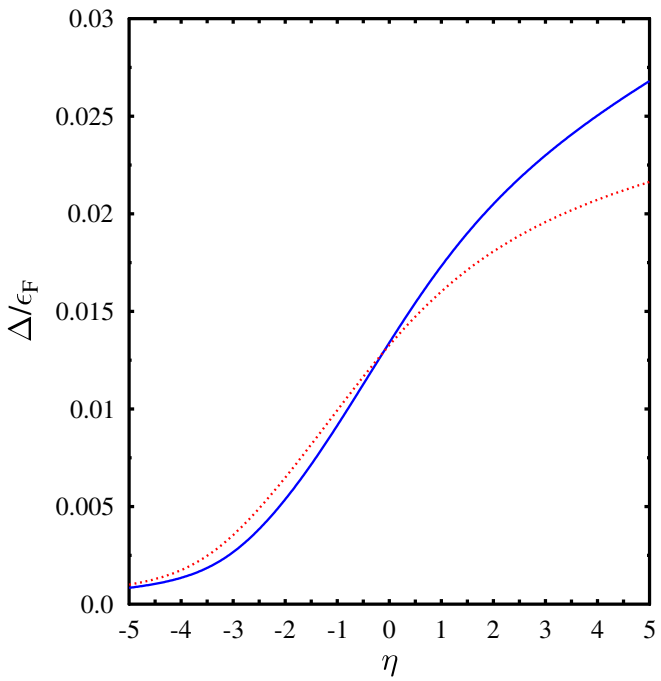

FIG. 1 (color online). Gap parameter in units of Fermi energy is plotted as a function of the dimensionless coupling. The dotted line corresponds to the case where antiparticle contributions are not included. The solid line corresponds to the case with inclusion of the antiparticle contributions. In this plot, we have chosen $\Lambda/k_f = 50$ and $m/k_f = 5$.

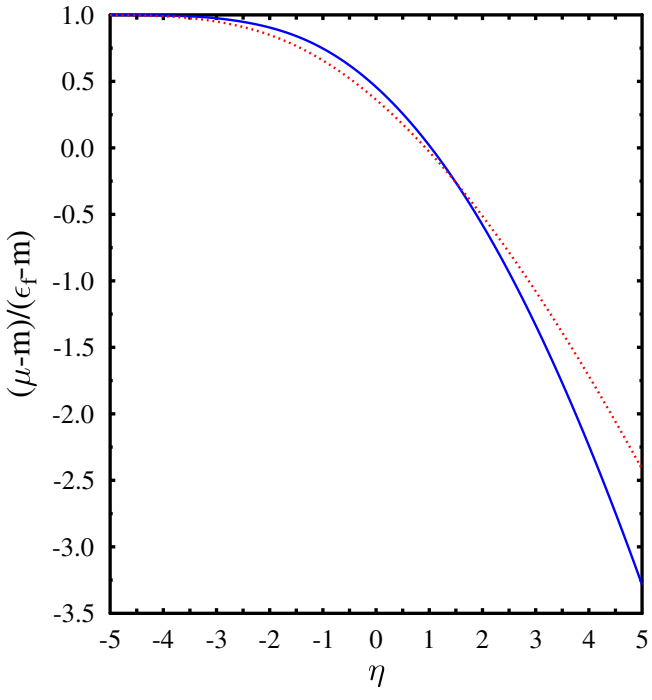

FIG. 2 (color online). The scaled chemical potential $(\mu - m)/(\epsilon_f - m)$ is plotted as a function of the dimensionless coupling η. The dotted line corresponds to the case where antiparticle contributions are not included. The solid line corresponds to the case with inclusion of the antiparticle contributions. In this plot, we have $\Lambda/k_f = 50$ and $m/k_f = 5$.

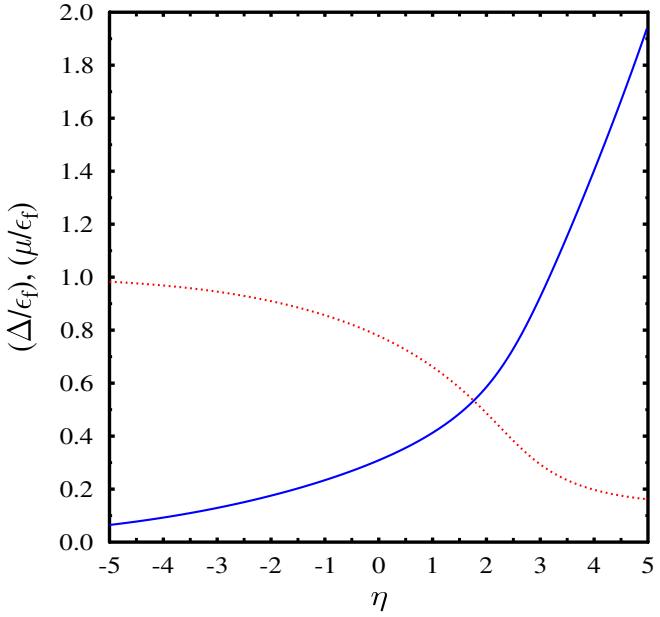

FIG. 3 (color online). Superfluid gap (solid line) and chemical potential (dotted line) in units of Fermi energy as functions of the dimensionless coupling η.

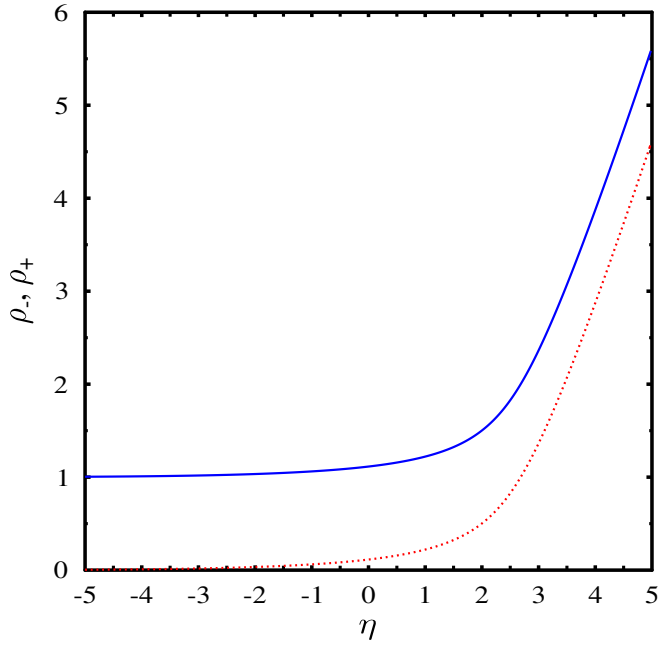

FIG. 4 (color online). Number densities of fermions ρ_- (solid line) and antifermions ρ_+ (dotted line) in units of $k_f^3/3\pi^2$ as a function of dimensionless coupling η.

the Fermi energy in a deep BEC regime of large positive value of η. The gap starts with exponentially small values in the weak coupling regime as expected from BCS theory and rises monotonically as the coupling increases. It becomes of the order of the Fermi energy at around the unitary regime $\eta = 0$. For $\eta = 0$, the superfluid gap and the chemical potential turn out to be $\Delta = 0.3\epsilon_f$ and $\mu = 0.78\epsilon_f$ respectively. We might note here that the same turns out to be about $\mu = 0.37\epsilon_f$ in Ref. [6]. The discrepancy between the two can easily be understood by comparing the gap equation in the unitary limit in the two cases. The difference lies in the way the renormalization of the gap equation is being done in these cases. To compare with the nonrelativistic results, we subtract out the mass terms from both the chemical potential as well as the Fermi energy. The resulting ratio then becomes $\tilde{\mu}/\tilde{\epsilon}_f = (\mu - m)/(\epsilon - m) \approx 0.5$. In the nonrelativistic fermionic models this value turns to be 0.4 to 0.5 [15,28–30]. As η increases, at about $\eta = 1.68$, the chemical potential becomes smaller than the mass of the fermion and the system goes to the BEC regime.

As the coupling becomes close to the unitary regime, the antifermion contributions become important. In Fig. 4, we show the number densities of the fermions ρ_- and the antifermions ρ_+ as defined in Eq. (38) and (39) respectively. While in the BCS regime the antiparticle contribution to the number density turns out to be negligible as compared to the particle contributions, where it becomes increasingly important near the unitary regime. At very large values of η, the chemical potential becomes negligible, the contributions of the particle and the antiparticle to the number densities become large as compared to the density ρ, and their difference produces a conserved net density [7].

Next, we consider the case of superfluid with a mismatch in the chemical potentials, i.e. $\delta_\mu \neq 0$. In the numerical calculations, we keep the average density fixed and calculate the average chemical potential and the superfluid gap using Eq. (37) and (36) respectively. The stability of the solution is analyzed by calculating the thermodynamic potential. Sometimes, particularly near the phase transition region, there are multiple solutions of the gap and number density equations. Of these, we choose the solution which has the least thermodynamic potential. We also numerically verify the positivity of second derivative of the thermodynamic potential at this pair of Δ and $\bar{\mu}$. This way we ensure that the solution we get is a minimum and not a maximum of the thermodynamic potential.

To analyze the nature of the solutions, we shall further assume, without loss of generality, $\delta_\mu > 0$. In that case, the quasiparticle energy for species 1 $\omega_-^{(1)}(\mathbf{k}) = \bar{\omega}_-(\mathbf{k}) - \delta_\mu$ and the same for quasiantiparticle energy of species 2 $\bar{\omega}_+^{(2)}(\mathbf{k}) = \bar{\omega}_+(\mathbf{k}) - \delta_\mu$ can become negative. In that case, at zero temperature the contributions of the Θ functions both in the gap equation (35) and the thermodynamic potential Eq. (34) can be nonvanishing. The Θ functions limit the range of the momentum integrations. Solving for the zeros of $\omega^{(1)}$, we note that this vanishes at momenta $\mathbf{k}^2_{\text{min/ max}} = (\bar{\mu} \pm \sqrt{\delta_\mu^2 - \Delta^2})^2 - m^2$. Similarly

$\omega_+^{(2)}$ vanishes at momenta satisfying $\mathbf{k}^2_{\mathrm{min/\,max}} = (-\bar{\mu} \pm \sqrt{\delta_\mu^2 - \Delta^2})^2 - m^2$. Clearly this is possible provided the gap Δ is smaller than δ_μ. The zeros of the dispersion relations correspond to effective Fermi surfaces. In general there can be two Fermi surfaces for species 1 along with the gapped ones. From the dispersion relations for the quasiparticles and antiparticles, it is clear that we also can have the interesting possibility of interior gap solutions for particles of species 1 and antiparticles of species 2 [6].

After these general remarks regarding the topology of Fermi surfaces, let us discuss some numerical results of the present investigation. As mentioned earlier, we keep the average density fixed and calculate the superfluid gap and the average chemical potential for a given coupling and a given chemical potential difference. In case there are multiple nontrivial solutions for the gap and the average chemical potential, the solution for the gap and average chemical potential pair is accepted which has the least thermodynamic potential.

In the numerical calculations that we present here, we take the parameters $\Lambda/k_f = 3.3$ and $m/k_f = 0.67$. In Fig. 5, we plot the quantity δ_μ^c/Δ, the ratio of maximum chemical potential difference to the superfluid gap, that can sustain pairing, as a function of the dimensionless coupling η. For a larger value of δ_μ, beyond δ_μ^c there are no acceptable solutions of the gap and number density equation with a nonvanishing gap and with a lower thermodynamic potential. For weak coupling in the BCS limit, it approaches the Clogston-Chandrasekhar limit of $\delta_\mu^c/\Delta \simeq 0.72$. Initially, as the coupling increases from BCS to BEC regime, δ_μ^c/Δ increases monotonically as shown by the solid line in Fig. 5. In this regime there are no gapless modes and the density difference δ_ρ between the two species is zero. At $\eta \simeq 1.9$, δ_μ^c/Δ increases sharply with η until it reaches a value of the order of 2.2. This is shown by the dotted line in Fig. 5. In this regime, $\omega^{(1)}$ becomes gapless while all other modes are gapped. In this region, $(\bar{\mu} - m)$ is negative and hence this gapless phase lies in the BEC regime. The density difference between the two species becomes nonzero. The dispersion relation $\omega^{(1)}(\mathbf{k})$ in this region is shown in Fig. 6. In particular we have chosen here $\eta = 2.2$ and $\delta_\nu/\Delta_0 = 0.47$. Here Δ_0 is the superfluid gap at zero chemical potential difference and turns out to be $\Delta_0 = 0.637\epsilon_f$. With these parameters, the average chemical potential turns out to be $\bar{\mu} = 0.47\epsilon_f$ and the gap is $\Delta \simeq 0.35\epsilon_f$.

The ratio δ_c/Δ increases with η till $\eta \simeq 2.5$. Beyond this, there are two gapless modes. Both the usual quasiparticle for species 1 and the quasiantiparticles of species 2 become gapless beyond this coupling. The dashed line in

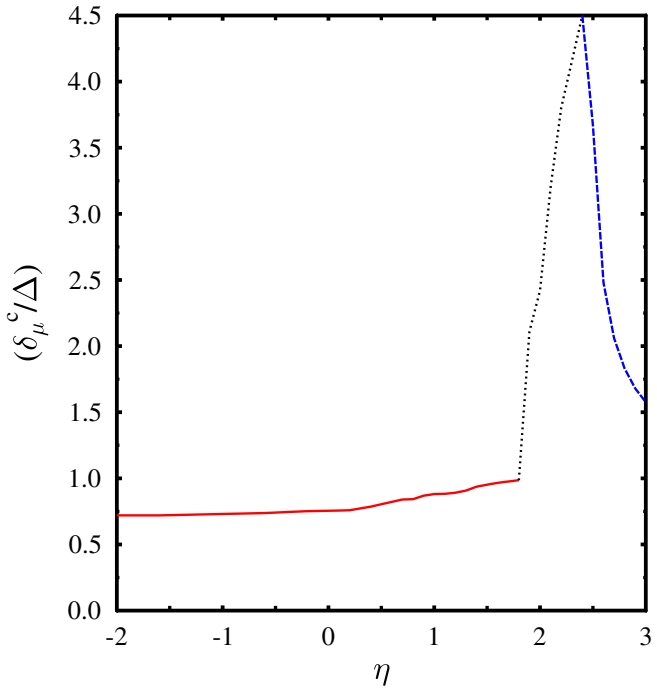

FIG. 5 (color online). Ratio of critical chemical potential difference to the gap as a function of the coupling strength η. Gapless phase appears for $\eta > 1.9$. Solid line denotes the BCS regime and the dotted line indicates the regime where quasiparticles of species 1 become gapless. The dashed line indicates the regime where the antiparticles of species 2 also become gapless.

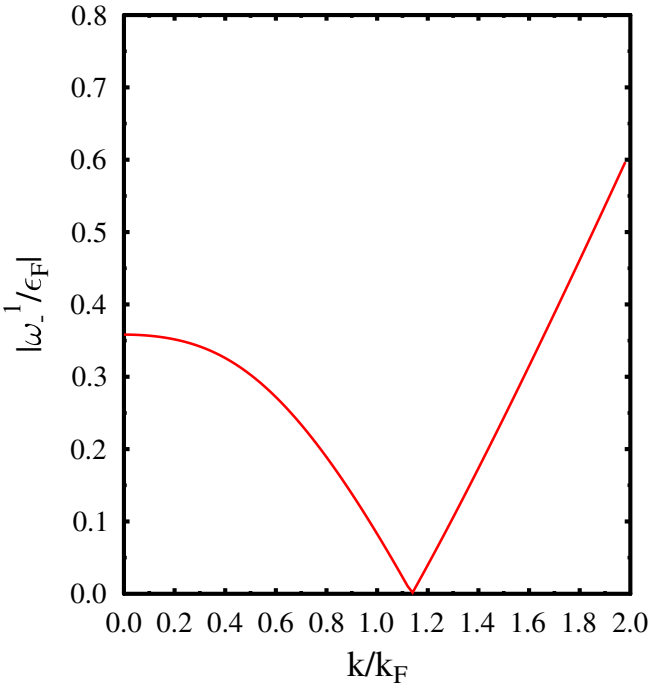

FIG. 6 (color online). Quasiparticle dispersion relation for species 1. The plot is for the case of coupling $\eta = 2.1$ and chemical potential difference $\delta/\Delta_0 = 1.125$, Δ_0 being the gap at zero chemical potential difference.

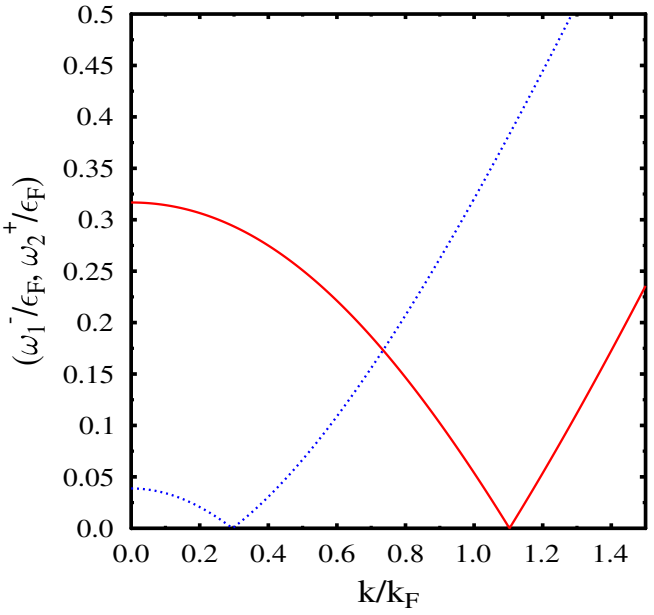

FIG. 7 (color online). Dispersion relation for gapless modes. Solid line shows the dispersion relation for quasiparticle of species 1($\omega_{-}^{(1)}(\mathbf{k})$) and the dotted line shows the dispersion relation for quasiantiparticle of species 2 ($\omega_{+}^{(2)}(\mathbf{k})$). The plot is for the case of coupling $\eta = 3$ and $\delta_\nu/\Delta_0 = 1.195$.

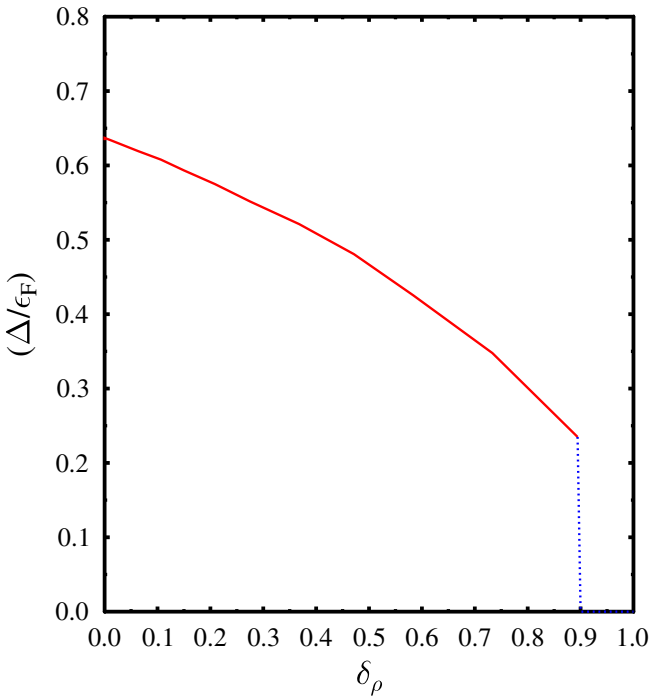

FIG. 8 (color online). Superfluid gap as a function of difference in number densities of the condensing species. This is plotted for $\eta = 2.1$.

Fig. 5 represents this regime. In Fig. 7 we show the dispersion relation for these gapless modes. We have taken the coupling $\eta = 3$ and $\delta/\Delta_0 = 1.195$ here. The values for the gap and the average chemical potential here is $\Delta = 0.72\epsilon_f$ and $\bar{\mu} = 0.23\epsilon_f$ respectively.

We also would like to note here that we did not find any breached pairing, i.e., two Fermi surfaces with nonzero value of the gap for any value of the coupling η. These results are similar qualitatively to those of Ref. [6] where a different renormalization was adopted for the crossover parameter.

We might mention here that we do not keep the density difference fixed in our calculations. We perform the calculations for a fixed average density and a given chemical potential difference. In the presence of gapless phases, the density difference becomes nonzero. In Fig. 8, the dependence of the gap on the density difference δ_ρ is shown for coupling $\eta = 2.1$. Superconductivity is supported for a maximum density difference of $\delta_\rho \simeq 0.9(k_f^3/3\pi^2)$ beyond which the system goes over to normal matter with zero gap. For coupling $\eta < 1.9$ we do not find any superfluid phase free energetically favorable with any nonzero value of density difference δ_ρ. However, a chemical potential difference can still support a Cooper paired state.

Next, let us consider the number density distribution of the two species in the momentum space when gapless modes exist. Let us note that the number densities at zero temperature for the two species are given by

$$\begin{aligned}\rho_1 &= \langle \psi_1^\dagger \psi_1 \rangle \\ &= \frac{2}{(2\pi)^3}\int d\mathbf{k}(\sin^2 f(\mathbf{k}) + \Theta(-\omega_{-}^{(1)})\cos^2 f(\mathbf{k}) \\ &\quad - \sin^2 f_1(\mathbf{k})(1 - \theta(-\omega_{+}^{(2)}))) \\ &\equiv \frac{2}{(2\pi)^3}\int d\mathbf{k} n_1(\mathbf{k}) \end{aligned} \tag{46}$$

for species 1 and

$$\begin{aligned}\rho_2 &= \langle \psi_2^\dagger \psi_2 \rangle \\ &= \frac{2}{(2\pi)^3}\int d\mathbf{k}(\sin^2 f(\mathbf{k})(1 - \Theta(-\omega_{-}^{(1)})) \\ &\quad - (\sin^2 f_1(\mathbf{k}) + \cos^2 f_1(\mathbf{k})\theta(-\omega_{+}^{(2)}))) \\ &\equiv \frac{2}{(2\pi)^3}\int d\mathbf{k} n_2(\mathbf{k}) \end{aligned} \tag{47}$$

for species 2. Here, $\tan 2f(\mathbf{k}) = \Delta/\bar{\xi}_-$ and $\tan 2f_1(\mathbf{k}) = \Delta/\bar{\xi}_+$. In Fig. 9 we have plotted the momentum space density distributions $n_1(\mathbf{k})$ and $n_2(\mathbf{k})$ for $\eta = 3.0$ and $\delta_\nu/\Delta_0 = 1.195$. In this case both $\omega_{-}^{(1)}$ and $\omega_{+}^{(2)}$ become gapless. In the region where both $\omega_{-}^{(1)}$ and $\omega_{+}^{(2)}$ are negative, $n_1(k) = 1$ and $n_2(k) = -1$ as may be seen from Eqs. (46) and (47). In the region where only $\omega_{-}^{(1)}$ is negative, $n_1(k) = (1 + \bar{\xi}_+/\bar{\omega}_+)/2$ and $n_2(k) = -(1 + \bar{\xi}_+/\bar{\omega}_+)/2$. Finally, when both $\omega_{-}^{(1)}$ and $\omega_{+}^{(2)}$ are positive,

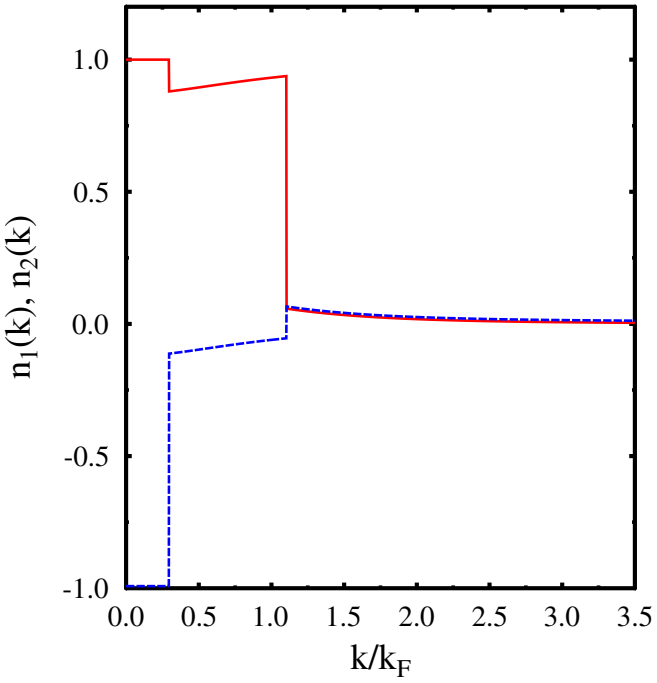

FIG. 9 (color online). Number density distribution for the two species. Solid line corresponds to species 1 and the dashed line corresponds to species 2. This plot corresponds to $\eta = 3.0$ and $\delta_\mu/\Delta_0 = 1.195$.

both $n_1(k)$ and $n_2(\mathbf{k})$ are identical and are given by the relativistic BCS distribution function $n(\mathbf{k}) = (\bar{\xi}_+/\bar{\omega}_+ - \bar{\xi}_-/\bar{\omega}_-)$. This is precisely what is depicted in Fig. 9. Let us note here that although the individual distribution functions in the momentum space for the two species could be negative, the average occupation number densities $\bar{n}(\mathbf{k}) = (n_1(\mathbf{k}) + n_2(\mathbf{k}))/2$ as well as the difference in occupation number densities $\delta_n(\mathbf{k}) = (n_1(\mathbf{k}) - n_2(\mathbf{k}))/2$ are always positive definite.

Most of the results obtained in this section for the model with a four-fermion interaction are similar to the mean field results obtained in a boson-fermion model [6]. It is nice to see the similarity to the mean field results of Ref. [6] which in our investigation arises with a simple ansatz for the ground state given by of Eq. (9) determined through an extremization of the thermodynamic potential. As emphasized in Sec. II, the scalar condensate field was considered as a classical auxiliary field. In the following section we shall treat them as dynamical fields and generalize the ansatz of Eq. (9) to include the quanta of this field along with those of the fermions. We shall illustrate this for the symmetric case, i.e. when there is no chemical potential mismatch for the two species of fermions.

IV. DYNAMICAL CONDENSATE FIELDS AND GENERALIZATION OF THE BCS ANSATZ

As discussed earlier, we shall now treat the scalar filed Φ introduced in Eq. (3) as a dynamical field and rewrite the Lagrangian as

$$\mathcal{L} = \mathcal{L}_f + \mathcal{L}_b + \mathcal{L}_{bf}, \tag{48}$$

where

$$\mathcal{L}_f = \bar{\psi}^i(i\gamma^\mu\partial_\mu - m + \mu\gamma^0)\psi^i, \tag{49}$$

$$\mathcal{L}_b = (\partial_0 - i\mu_B)\Phi^\dagger(\partial_0 + i\mu_B)\Phi - m_b^2\Phi^\dagger\Phi - (\nabla\Phi^\dagger)(\nabla\Phi) - \lambda(\Phi^\dagger\Phi)^2, \tag{50}$$

and

$$\mathcal{L}_{bf} = g|\epsilon^{ij}|(\bar{\psi}^i\gamma^5\psi_c^j\Phi + \bar{\psi}_c^i\gamma^5\psi^j\Phi^*). \tag{51}$$

We shall illustrate the effect of the dynamical bosonic field on the BCS-BEC crossover physics and hence will consider the case where there is no mismatch in the chemical potentials of the two condensing fermionic species with a common chemical potential μ. For the dynamical bosonic field now we have introduced the chemical potential μ_B which is equal to twice the fermionic chemical potential μ in equilibrium. We have also included a quartic term in the scalar field in $\mathcal{L}_B$ for the sake of completeness. In fact, this quartic term leads to nonperturbative corrections to the thermodynamic potential as we shall observe later. Clearly, in the absence of the kinetic terms and the quartic interaction term, this Lagrangian reduces to the one considered in Sec. II.

As before, we shall consider a state such that $\langle\Phi\rangle = \phi_0 = \langle\Phi^\dagger\rangle$ and investigate the fluctuations of the condensate field by defining the quantum fields $\Phi' = \Phi - \phi_0$ and $\Phi'^\dagger = \Phi^\dagger - \phi_0$. Then $\mathcal{L}_b$ reduces to

$$\mathcal{L}_b \simeq (\partial_0 - i\mu_B)\Phi'^\dagger(\partial_0 + i\mu_B)\Phi' - m_b^2\Phi'^\dagger\Phi' - (\nabla\Phi'^\dagger)(\nabla\Phi') - \lambda(\Phi'^\dagger\Phi')^2 - 4\lambda\phi_0^2(\Phi'^\dagger\Phi') - V_0(\phi_0), \tag{52}$$

where $\simeq$ means neglecting odd powers in Φ's. Further, in the above, $V_0(\phi_0)$ is the tree level potential given as

$$V_0(\phi_0) = (m_b^2 - \mu_B^2)\phi_0^2 + \lambda\phi_0^4. \tag{53}$$

One can write down the corresponding Hamiltonian densities as

$$\mathcal{H} = \mathcal{H}_f + \mathcal{H}_b + \mathcal{H}_{bf} \tag{54}$$

with

$$\mathcal{H}_f = \sum_i \psi_i^\dagger(-i\alpha\cdot\nabla + \beta m)\psi_i \tag{55}$$

$$\mathcal{H}_b = \Pi_{\Phi'^\dagger}\Pi_{\Phi'} + i\mu_b(\Pi_{\Phi'}\Phi' - \Pi_{\Phi'^\dagger}\Phi'^\dagger) + \Phi'^\dagger(-\nabla^2 + m_b^2)\Phi' + \lambda(\Phi'^\dagger\Phi')^2 + 4\lambda\phi_0^2(\Phi'^\dagger\Phi') + V_0(\phi_0) \tag{56}$$

and $\mathcal{H}_{bf} = -\mathcal{L}_{bf}$. Here, $\Pi_{\Phi'}$ ($\Pi_{\Phi'^\dagger}$) is the conjugate

momentum of the corresponding field Φ' ($\Phi'^{\dagger}$). Similar to the fermion field operator expansion we can take the boson field operator expansions in terms of creation and annihilation operators. We have thus e.g.

$$\Phi'(\mathbf{x}, t=0) = \frac{1}{(2\pi)^{3/2}} \int d\mathbf{k} \frac{1}{\sqrt{2\omega(k)}} \times (a(\mathbf{k}) + b^{\dagger}(-\mathbf{k}))e^{i\mathbf{k}\cdot\mathbf{x}} \quad (57)$$

and

$$\Pi_{\Phi'}(\mathbf{x}, t=0) = \frac{i}{(2\pi)^{3/2}} \int d\mathbf{k} \sqrt{\frac{\omega(k)}{2}} \times (-b(\mathbf{k}) + a^{\dagger}(-\mathbf{k}))e^{i\mathbf{k}\cdot\mathbf{x}}. \quad (58)$$

Let us note that with the above expansion for the conjugate fields satisfying the quantum algebra $[\Phi'(\mathbf{x}), \Pi_{\Phi'}(\mathbf{y})] = i\delta(\mathbf{x}-\mathbf{y})$ leads to the usual commutation relations for the creation and annihilation operators $[a(\mathbf{k}), a^{\dagger}(\mathbf{k}')] = \delta(\mathbf{k}-\mathbf{k}') = [b(\mathbf{k}), b^{\dagger}(\mathbf{k}')]$ for *any arbitrary function* $\omega(\mathbf{k})$.

With the operators for the scalar fields defined, we now generalize the ansatz given in Eq. (9) and write down the ansatz $|\Omega(\beta, \mu\rangle_B$ to include the effects of the boson field as

$$|\Omega(\beta, \mu)\rangle_B = \mathcal{U}^B_{\beta,\mu} U^B |\Omega(\beta, \mu)\rangle. \quad (59)$$

Here, similar to Eq. (9) and (8) the operator U^B is given as

$$U^B = \exp\left(\int d\mathbf{k} g(k) a^{\dagger}(\mathbf{k}) b^{\dagger}(-\mathbf{k}) - \text{H.c.}\right) \quad (60)$$

and similar to Eq. (10) and (11), the operator corresponding to thermal excitations of the bosonic fields $\mathcal{U}^B_{\beta}\mu$ is given as

$$\mathcal{U}^{\ B}_{\beta\mu} = \exp\left(\int d\mathbf{k} (a'^{\dagger}(\mathbf{k}) \underline{a}(-\mathbf{k}) \theta_a(\mathbf{k}, \mu) + b'^{\dagger}(\mathbf{k}) \underline{b}(-\mathbf{k}) \theta_b(\mathbf{k}, \mu)) - \text{H.c}\right). \quad (61)$$

This leads to e.g.

$$\langle \Phi'(\mathbf{x}) \Phi'(\mathbf{y}) \rangle = \frac{1}{(2\pi)^3} \int \frac{d\mathbf{k}}{2\omega(\mathbf{k})} \times e^{i\mathbf{k}\cdot(\mathbf{x}-\mathbf{y})} [(\cosh 2g(\mathbf{k}) + \sinh 2g(\mathbf{k})) \times (\cos h^2\theta^a + \sin h^2\theta^b)] \equiv I(\mathbf{x}-\mathbf{y}, \beta), \quad (62)$$

where the expectation value is taken with respect to the state $|\Omega(\beta, \mu)\rangle_B$ defined in Eq. (59). The extra functions $g(\mathbf{k})$ as well as the thermal bosonic functions $\theta^{a,b}$ are to be determined as earlier by extremization of the thermodynamic potential. The thermodynamic potential for the boson-fermion system can be written as

$$\Omega_{\text{tot}} = \Omega + \Omega_B. \quad (63)$$

Here, the fermionic contribution Ω has already been evaluated in Eq. (23). The bosonic contribution Ω_B is given by

$$\Omega_B = \epsilon_B - \mu_B \rho_B - \frac{1}{\beta} s_B. \quad (64)$$

The contribution of the first two terms is just the expectation value of Eq. (56) with respect to the state in Eq. (60). The bosonic entropy density s_B is given similar to their fermionic counterpart in Eq. (28), as [25]

$$s_B = \frac{1}{(2\pi)^3} \sum_i \int d\mathbf{k} (\cosh^2\theta_a \ln\cosh^2\theta_a - \sinh^2\theta_a \ln\sinh^2\theta_a + a \rightarrow b). \quad (65)$$

Extremization of the total thermodynamical potential with respect to the fermionic functions $f(\mathbf{k})$, $f_1(\mathbf{k})$, and $\theta^i_{\mp}(\mathbf{k})$ leads to the same solutions for them as given in Sec. II B. Extremizing the bosonic function $g(\mathbf{k})$ leads to the solution

$$\tanh 2g(k) = \frac{\omega^2 - \mathbf{k}^2 - M^2}{\omega^2 - \mathbf{k}^2 + M^2}, \quad (66)$$

with the quantity M^2 satisfying the temperature dependent mass gap equation given as

$$M^2 = m^2 + 4\lambda\phi_0^2 + \frac{4\lambda}{(2\pi)^3} \int \frac{d\mathbf{k}}{2\sqrt{\mathbf{k}^2 + M^2}} \times (\cosh^2\theta_a + \sinh^2\theta_b) = m^2 + 4\lambda(\phi_0^2 + I(\beta)). \quad (67)$$

Here, $I(\beta) = I(\mathbf{0}, \beta)$ as given in Eq. (62). Similarly, minimizing the thermodynamic potential with respect to the bosonic thermal functions yields

$$\sinh^2\theta_a = \frac{1}{\exp(E_B - \mu_B) - 1} \equiv n_B(\mathbf{k}) \quad (68)$$

for the boson particle distribution function and

$$\sinh^2\theta_b = \frac{1}{\exp(E_B + \mu_B) - 1} \equiv n_{\bar{B}}(\mathbf{k}) \quad (69)$$

for the boson antiparticle distribution function and $E_B = \sqrt{\mathbf{k}^2 + M^2}$, with the temperature dependent mass M satisfying the self-consistent mass gap equation (67).

With all the functions in the ansatz state [Eq. (59)] now determined, the total thermodynamic potential can be written, using Eqs. (34) and (63), as

$$\Omega_{\text{tot}} = \Omega_f + \Omega_B, \quad (70)$$

where the fermionic part of the thermodynamic potential is given by

$$\Omega_f = \frac{2}{(2\pi)^3}\int(2\epsilon(k) - \bar{\omega}_- - \bar{\omega}_+)d\mathbf{k} - \frac{2}{(2\pi)^3\beta}\sum_i\int d\mathbf{k}[\ln(1 + e^{(-\beta\omega_-^{(i)})}) + \ln(1 + e^{(-\beta\omega_+^{(i)})})]. \quad (71)$$

As compared to expression in Eq. (34), the above differs by the mass term $m_b^2\phi_0^2$ which is absorbed naturally in the bosonic part of the thermodynamic potential and the latter is given as

$$\Omega_B = \frac{1}{(2\pi)^3}\int d\mathbf{k}\sqrt{\mathbf{k}^2 + M^2} - 2\lambda I^2(\beta) + \frac{1}{\beta(2\pi)^3}\int d\mathbf{k}\sum_{i=1}^{2}\ln(1 - \exp(E_i)) + V_0, \quad (72)$$

where the summation is over the bosons and antibosons with $E_1 = E_B - \mu_B$, $E_2 = E_B + \mu_B$, and V_0 is the tree level potential

$$V_0 = (m_b^2 - \mu_B^2)\phi_0^2 + \lambda\phi_0^4. \quad (73)$$

Finally, the extremization of the total thermodynamic potential with respect to ϕ_0 leads the superconducting gap equation

$$M^2 - \mu_B^2 = 2\lambda\phi_0^2 + 4g^2\int\frac{d\mathbf{k}}{(2\pi)^3}\left[\frac{\cos2\theta_-^{1,2}}{\bar{\omega}_-} + \frac{\cos2\theta_+^{1,2}}{\bar{\omega}_+}\right], \quad (74)$$

with, the mass M satisfying the mass gap equation (67) and $\cos2\theta_\mp^{1,2} = (1 - \sin^2\theta_\mp^1(\mathbf{k}) - \sin^2\theta_\mp^2(\mathbf{k}))$ with $\sin^2\theta_\pm^i(\mathbf{k})$ being the thermal distribution functions for the fermions defined in Eq. (31). This is the parallel of Eq. (35) where the condensate field was considered as an auxiliary field and there was no quartic coupling term for the scalar field.

The expression for the bosonic part of the thermodynamic potential Ω_B in Eq. (72) is, however, affected by two types of divergences, one arising from the divergent integrals as vacuum terms ($\phi_0 = 0$ at $T = 0$, $\mu = 0$) which are still to be subtracted and the other being the fact that the mass parameter M^2 is not well-defined because of the infinities in the mass gap equation (67). This can be taken care of by defining the renormalized quartic coupling and the boson mass through the relations [21,22]

$$\frac{1}{\lambda_R} = \frac{1}{\lambda} + 4I_2(\Lambda, \mu_{sc}), \quad (75)$$

$$\frac{m_R^2}{\lambda_R} = \frac{m_b^2}{\lambda} + 4I_1(\Lambda, \mu_{sc}), \quad (76)$$

where I_1 and I_2 are divergent integrals evaluated with a three-momentum cutoff defined as

$$I_1 = \frac{1}{(2\pi)^3}\int^{|\mathbf{k}|<\Lambda}\frac{d\mathbf{k}}{2|\mathbf{k}|} = \lim_{\Lambda\to\infty}\frac{\Lambda^2}{8\pi^2} \quad (77)$$

and

$$I_2 = \frac{1}{\mu_{sc}^2(2\pi)^3}\int^{|\mathbf{k}|<\Lambda}d\mathbf{k}\left(\frac{1}{2|\mathbf{k}|} - \frac{1}{2\sqrt{\mu_{sc}^2 + \mathbf{k}^2}}\right) = \frac{1}{16\pi^2}\left(\ln\left(\frac{4\Lambda^2}{\mu_{sc}^2}\right) - 1\right), \quad (78)$$

where μ_{sc} is the renormalization scale and Λ is the three-momentum cutoff. Using the renormalization parameters the mass gap equation can be written in terms of finite quantities as

$$M^2 = m_R^2 + 4\lambda_R(\phi_0^2 + I_f(\beta)), \quad (79)$$

with $I_f(\beta)$ given as

$$I_f(\beta) = \frac{M^2}{16\pi^2}\left(\ln\left(\frac{M^2}{\mu_{sc}^2}\right) + 1\right) + \int\frac{d\mathbf{k}}{(2\pi)^3}\frac{1}{2E}(n_B(\mathbf{k}) + n_{\bar{B}}(\mathbf{k})). \quad (80)$$

Similarly the bosonic part of the effective potential Eq. (72) in terms of the renormalized parameters, subtracting out the vacuum terms, becomes finite and is given as

$$\Omega_B = V_0 + V_1 + V_2 \quad (81)$$

with

$$V_0 = m_R^2\phi_0^2 + \lambda_R\phi_0^4 - \mu_B^2\phi_0^2 + (\lambda_R - \lambda)\phi_0^4, \quad (82)$$

$$V_1 = \frac{1}{\beta(2\pi)^3}\int d\mathbf{k}\sum_{i=1}^{2}\ln(1 - \exp(E_i)) + \frac{M^4}{32\pi^2}\ln\left(\frac{M^2}{\mu_{sc}^2}\right), \quad (83)$$

and

$$V_2 = -2\lambda_R I_f(\beta)^2. \quad (84)$$

The cutoff dependence in the effective potential is still there in the last term of Eq. (82) which disappears in the limit of $\Lambda \to \infty$ as the bare coupling λ vanishes in that limit. In the present calculations, however, we keep the cutoff finite. We might note here that the difference between the bare and the renormalized quartic coupling can be written as

$$\lambda - \lambda_R = \frac{4\lambda_R I_2(\Lambda, \mu_{sc})}{1 - 4\lambda_R I_2(\Lambda, \mu_{sc})}\lambda_R, \quad (85)$$

where I_2 is given in Eq. (78). Mostly in our numerical calculations we shall have the limit $4\lambda_R I_2 << 1$, in which case, the contribution of the last term in Eq. (82) is negligible.

Next, the fermionic part of the thermodynamic potential Eq. (71) and the terms V_0, V_2 of the bosonic part can be combined using the gap equation (74) to yield a form similar to Eq. (41) as

$$\Omega_f^1 \equiv \Omega_f + V_0 + V_2$$
$$= \frac{2}{(2\pi)^3\beta}\int d\mathbf{k}\Bigg[\Bigg(\bar{\xi}_- - \bar{\omega}_- + \frac{\Delta^2}{2\bar{\omega}_-} + \bar{\xi}_+ - \bar{\omega}_+ + \frac{\Delta^2}{2\bar{\omega}_+}\Bigg) - \sum_i \{\ln(1+e^{(-\beta\omega_-^{(i)})}) + \ln(1+e^{(-\beta\omega_+^{(i)})})\}\Bigg] - \lambda_R\phi_0^4 - (\lambda_R - \lambda)\phi_0^4 - 2\lambda_R I_f(\beta)^2. \quad (86)$$

The number density equation (37) now gets modified due to the presence of dynamical condensate fields having a chemical potential twice that of the fermions and the number density equation becomes

$$\bar{\rho} = 8\mu\phi_0^2 + 2\int \frac{d\mathbf{k}}{(2\pi)^3}(\sinh^2\theta_a - \sinh^2\theta_b) + \frac{1}{(2\pi)^3}\int\Bigg[\frac{\xi_+}{\bar{\omega}_+}\cos 2\theta_+^{1,2} - \frac{\xi_-}{\bar{\omega}_-}\cos 2\theta_-^{1,2}\Bigg]d\mathbf{k}. \quad (87)$$

To discuss the crossover, we define the mass parameter m_1 as in Ref. [6] as

$$m_1^2 = m_R^2 - 4g^2\int \frac{d\mathbf{k}}{(2\pi)^3}\frac{2}{\sqrt{\mathbf{k}^2 + m^2}} \quad (88)$$

and define the crossover parameter as

$$x = -\frac{m_1^2 - \mu_B^2}{4g^2}. \quad (89)$$

The gap equation (74) becomes

$$m_1^2 - \mu_B^2 = 2(\lambda - \lambda_R)\phi_0^2 - 2\lambda_R\phi_0^2 - 4\lambda_R I_f(\beta) + 4g^2\int\frac{d\mathbf{k}}{(2\pi)^3}\Bigg[\frac{\cos 2\theta_-^{1,2}}{\bar{\omega}_-} + \frac{\cos 2\theta_+^{1,2}}{\bar{\omega}_+} - \frac{2}{\sqrt{\mathbf{k}^2 + m^2}}\Bigg]. \quad (90)$$

Let us note here that the superfluid gap equation has now contributions from the bosonic fluctuations through the contribution $I_f(\beta)$. For numerical calculations, we choose a given value of the bosonic mass parameter m_R and solve the coupled number density equation and the superfluid gap equation (90) for the chemical potential and the superfluid gap. At each stage of evaluation of the right-hand side of Eq. (87) and (90), the boson mass parameter M^2 is calculated self-consistently solving Eq. (79). Throughout the numerical calculations we have chosen $g = 2\sqrt{2}$ and cutoff scale $\mu_{sc}^2 = m_R^2$. This way we obtain the superfluid gap and the chemical potential for a given value of m_R or equivalently, for a given value of x obtained through Eqs. (88) and (89). These are then used to calculate any other thermodynamical quantities. In Fig. 10, we show the numerical solutions of such a calculation for the gap and the chemical potential for zero temperature as a function of the dimensionless order parameter x/x_0 with $x_0 = \Lambda^2/(4\pi^2)$ for three values of the quartic coupling $\lambda_R =$ 0, 0.5, and 2.0. $\lambda = 0$ will correspond to the mean field results. As we might observe, the effects of the bosonic fluctuations are almost negligible in the BCS regime ($x/x_0 < 0$) as well as near the unitary regime ($x/x_0 \sim 0$). The effects of the fluctuating field are seen at large values of the crossover parameter in the deep BEC regime, manifesting in a small reduction of the superfluid gap. The magnitude of this reduction increases with the quartic coupling. This is due to the following reason. It is clear from observing the gap equation (90) that the effect of the positive quartic coupling leads to an increase in the bosonic chemical potential for the same value of the gap parameter. This leads to an increase of the corresponding value of the crossover parameter x as may be clear from Eq. (89) for the same superfluid gap parameter. This is also reflected in the number densities of the fermions and bosons which we show in Fig. 11. The change in chemical potential and the

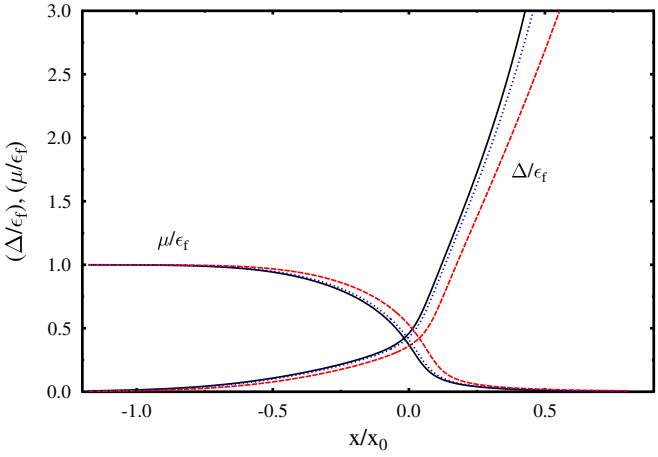

FIG. 10 (color online). Fermion chemical potential and gap in units of Fermi energy as a function of dimensionless crossover parameter x/x_0. The solid, dotted, and dashed curves correspond to $\lambda_R = 0$, 0.5, and 2, respectively.

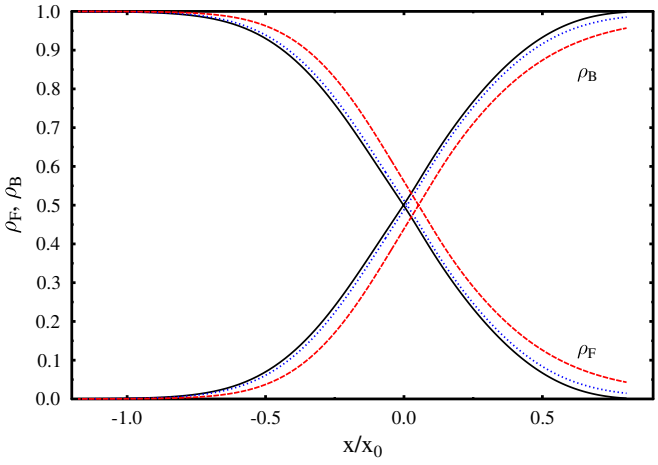

FIG. 11 (color online). Number densities of fermions and bosons in units of total number density. The solid, dotted, and the dashed curves correspond to $\lambda_R = 0$, 0.5, and 2, respectively.

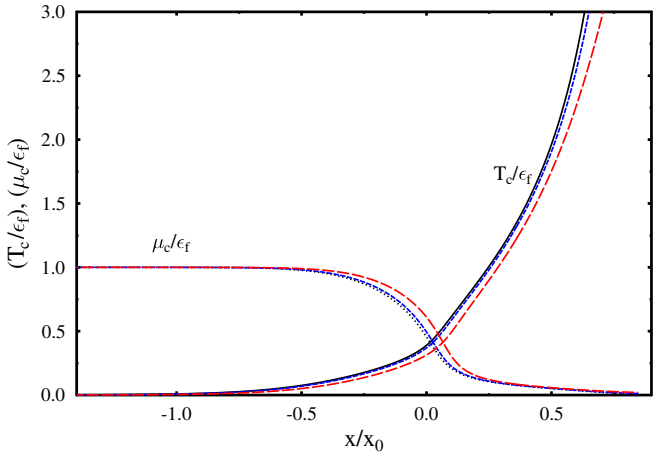

FIG. 12 (color online). Critical temperature T_c and the chemical potential at $T = T_c$ in units of Fermi energy as a function of dimensionless crossover parameter. The solid, dotted, and dashed curves correspond to $\lambda_R = 0$, 0.5, and 2, respectively.

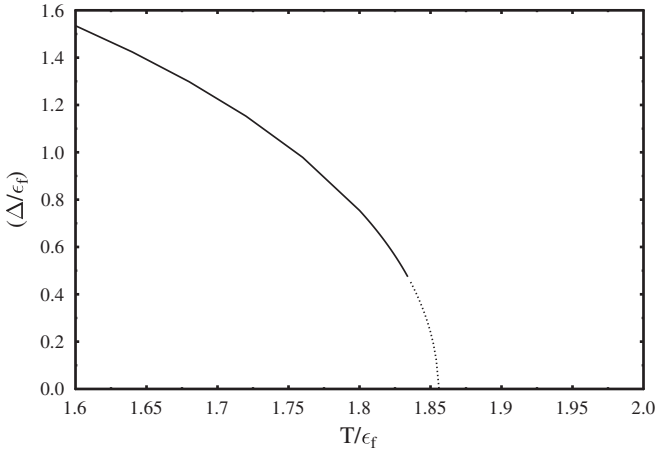

FIG. 13. Superfluid gap as a function of temperature for quartic coupling $\lambda_R = 5$. The dotted line corresponds to unstable solutions which are to solutions of the gap equation but with a higher thermodynamic potential as compared to $\Delta = 0$.

gap is appreciable from their corresponding mean field values only in the BEC regime.

We then present the results for the critical temperature and the chemical potential as a function of the crossover parameter. This is done by setting $\Delta = 0 = \phi_0$ in the number density equation (87), in the gap equation (90) as well as in the mass gap equation (79). The results are shown in Fig. 12. While the behavior of the chemical potential is qualitatively similar to that at zero temperature, the critical temperature behaves similarly to the gap at zero temperature with the crossover parameter. The correction to the critical temperature becomes significant in the BEC regime only and increases with the quartic coupling. In this case, again the reduction of the critical temperature occurs because of the increase in chemical potential due to thermal as well as vacuum fluctuations as may be seen in Eq. (90). With a further increase of the quartic coupling, the critical temperature become less and less steep due to larger contributions of the thermal fluctuation of the bosonic field.

To see the effect of the fluctuations of the condensate field we also looked into the behavior of the gap as a function of the temperature for different values of the quartic coupling parameter λ_R. As the magnitude of the quartic coupling is increased, it was observed that the order parameter Δ changes discontinuously at the critical temperature. A typical behavior for the solution of gap equation (90) is shown in Fig. 13 for $\lambda_R = 5$. We note that near the critical temperature there are solutions to the gap equation but having larger values of the thermodynamic potential as compared to the normal matter. This is suggestive of a first-order phase transition when the effect of fluctuations becomes large. One should however be careful in drawing conclusions from extrapolation to such a large value of the quartic coupling because, although the result here is nonperturbative, it is limited by the ansatz for the ground state in Eq. (59). In this context we might remark here that gauge field fluctuations in color superconductors change the superconducting phase transition to a first-order transition [31]. Similar observations were also made in Ref. [11] in a fermion-boson model where the fluctuations were treated within a CJT formulation.

V. SUMMARY

We have considered here a variational approach to discuss the ground state structure of a system of two species of relativistic fermions with a mismatch in their Fermi momenta. An explicit construct for the ground state is considered to describe the two fermion condensates. The ansatz functions including the distribution functions are determined by an extremization of the thermodynamic potential.

The quadratically divergent gap equation is made logarithmically divergent by subtracting out the vacuum contribution and the four-Fermi coupling is related to the s-wave scattering length as in Ref. [7,10]. Unlike the nonrelativistic case, the antiparticle degrees of freedom become important even for the case $k_f/m << 1$, particularly for large values of $\eta(\equiv 1/k_f a)$.

When the Fermi momenta of the two species are different, we do not observe any gapless modes in the BCS regime. A nonzero chemical potential difference can support a uniform BCS pairing with zero number density difference between the two species. Breached pairing solutions with two Fermi surfaces are also not observed. However, in the BEC region with $\bar{\mu} < m$, stable gapless modes are possible. The quasiparticle can become gapless for $\eta(\equiv 1/k_f a) > 1.9$ and, even for larger values of η, the quasiantifermions can also become gapless. Such gapless modes will be relevant for the transport coefficients of the fermionic system.

We have not calculated here the Meissner masses, or the number susceptibility to discuss the stability of different phases by ruling out regions in the parameter space of gap and chemical potential difference. Instead, we have solved the gap equation and the number density equation self-consistently and have compared the thermodynamic potentials. In certain regions of the chemical potential difference and the coupling, we have multiple solutions for the gap equation. In such cases, we have taken the solution which has the lowest thermodynamic potential, ensuring that it corresponds to a minimum. In the deep BEC region, the phase transition from BCS to gapless phase is a second-order phase transition with the order parameter decreasing continuously, while the transition from the gapless phase to the normal matter phase is a first-order transition as the difference in the densities of the two condensing species is increased.

The results obtained here are of course limited by the choice of the ansatz. We have not considered here other nonuniform ansatz leading to the Larkin-Ovchinnikov-Fulde-Ferrel (LOFF) phase or the crystalline phase [14,15,32,33]. The results obtained here might nevertheless be regarded as a reference solution with which other numerical or analytical results obtained from a more involved ansatz for the ground state may be compared. Though it is not *a priori* obvious, the results obtained through the simple variational ansatz for the ground state, regarding the phase structure for this purely fermionic theory, turn out to be similar to those of a Bose-Fermi model of Ref. [6] treated within a mean field approximation.

We have also considered the effects of the fluctuations by treating the condensate field as a dynamical bosonic field in a model with quartic self-interactions of the boson field. The BCS ansatz was modified to include the quanta of the fluctuating field along with the usual fermion pairs. Such an ansatz gave rise to a superfluid gap equation that includes the effect of condensate fluctuations. In the evaluation of the superconducting gap the scalar field mass gap was also calculated self-consistently. This leads to a decrease of the critical temperature in the BEC regime. We also observed that the superfluid transition could be first-order for larger quartic coupling with the effect of the condensate fluctuations becoming larger. The present ansatz for the ground state leads to the result arising from a summation of an infinite series of bubble diagrams for the scalar field. However, this does not include the effect of sunset type diagrams. Inclusion of such diagrams has been successfully done recently within a CJT formulation in Ref. [11].

We can generalize this toy model to a more realistic model like Nambu-Jona-Lasinio model, to describe the possibility of relativistic BCS-BEC crossover in quark matter phase diagram. Further, the effect of charge neutrality conditions, as appropriate for matter in the core of neutron stars, on relativistic BCS-BEC crossover will be important. Some of these calculations are in progress and will be reported elsewhere.

ACKNOWLEDGMENTS

H. M. would like to thank the organizers of the meeting on ''Interface of QGP and Cold Atoms'' at ECT*, Trento, and acknowledges discussions with D. H. Rischke, Y. Nishida, H. Abuki. A. M. would like to thank Frankfurt Institute for Advanced Studies (FIAS) for warm hospitality, where the present work was initiated and Alexander von Humboldt Foundation, Germany, for financial support during the visit. H. M. would also like to thank Institut fur Theoretische Physik, University of Frankfurt, for hospitality and Alexander von Humboldt Foundation for support. A. M. would like to acknowledge financial support from Department of Science and Technology, Government of India (Project No. SR/S2/HEP-21/2006).

[1] For reviews see M. G. Alford, A. Schmitt, K. Rajagopal, and T. Schaefer, arXiv:0709.4635; K. Rajagopal and F. Wilczek, arXiv:hep-ph/0011333; D. K. Hong, Acta Phys. Pol. B **32**, 1253 (2001); M. G. Alford, Annu. Rev. Nucl. Part. Sci. **51**, 131 (2001); G. Nardulli, Riv. Nuovo Cimento Soc. Ital. Fis. **25N3**, 1 (2002); S. Reddy, Acta Phys. Pol. B **33**, 4101 (2002); T. Schaefer arXiv:hep-ph/0304281; D. H. Rischke, Prog. Part. Nucl. Phys. **52**, 197 (2004); H. C. Ren, arXiv:hep-ph/0404074; M. Huang, arXiv: hep-ph/0409167; I. Shovkovy, arXiv:nucl-th/0410191.

[2] D. Bailin and A. Love, Phys. Rep. **107**, 325 (1984); D. Son, Phys. Rev. D **59**, 094019 (1999); T. Schaefer and F. Wilczek, Phys. Rev. D **60**, 114033 (1999); D. Rischke and R. Pisarski, Phys. Rev. D **61**, 051501 (2000); D. K. Hong, V. A. Miransky, I. A. Shovkovy, and L. C. Wiejewardhana, Phys. Rev. D **61**, 056001 (2000).

[3] H. Abuki, T. Hatsuda, and K. Itakura, Phys. Rev. D **65**, 074014 (2002).

[4] M. Kitazawa, D. Rischke, and I. A. Shovkovy, Phys. Lett. B **663**, 228 (2008).

[5] A. H. Rezaean and H. J. Pirner, Nucl. Phys. **A779**, 197 (2006).

[6] J. Deng, A. Schmitt, and Q. Wang, Phys. Rev. D **76**, 034013 (2007).

[7] G. F. Sun, L. He, and P. Zhuang, Phys. Rev. D **75**, 096004 (2007); L. He and P. Zhuang, Phys. Rev. D **76**, 056003 (2007).

[8] L. He and P. Zhuang, Phys. Rev. D **75**, 096003 (2007).

[9] Y. Nishida and H. Abuki, Phys. Rev. D **72**, 096004 (2005).
[10] H. Abuki, Nucl. Phys. **A791**, 117 (2007).
[11] J. Deng, J. Wang, and Q. Wang, Phys. Rev. D **78**, 034014 (2008).
[12] Tomas Brauner, Phys. Rev. D **77**, 096006 (2008).
[13] K. Rajagopal and A. Schmitt, Phys. Rev. D **73**, 045003 (2006).
[14] M. Mannarelli, G. Nardulli, and M. Ruggieri, Phys. Rev. A **74**, 033606 (2006).
[15] A. Mishra and H. Mishra, arXiv:cond-mat/0611058.
[16] H. Mishra and J. C. Parikh, Nucl. Phys. **A679**, 597 (2001).
[17] Amruta Mishra and Hiranmaya Mishra, Phys. Rev. D **69**, 014014 (2004).
[18] A. Mishra and H. Mishra, Phys. Rev. D **71**, 074023 (2005).
[19] B. Deb, A. Mishra, H. Mishra, and P. Panigrahi, Phys. Rev. A **70**, 011604(R) (2004).
[20] A. Mishra and H. Mishra, Phys. Rev. D **74**, 054024 (2006).
[21] G. Amelino-Camelia and S. Y. Pi, Phys. Rev. D **47**, 2356 (1993).
[22] D. Rischke and J. Lenaghan, J. Phys. G **26**, 431 (2000).
[23] A. Mishra and S. P. Misra, Z. Phys. C **58**, 325 (1993).
[24] H. Mishra and S. P. Misra, Phys. Rev. D **48**, 5376 (1993).
[25] H. Umezawa, H. Matsumoto, and M. Tachiki, *Thermofield Dynamics and Condensed States* (North-Holland, Amsterdam, 1982); P. A. Henning, Phys. Rep. **253**, 235 (1995).
[26] Amruta Mishra and Hiranmaya Mishra, J. Phys. G **23**, 143 (1997).
[27] C. A. R. Sa de Melo, M. Randeria, and J. R. Engelbrecht, Phys. Rev. Lett. **71**, 3202 (1993).
[28] S. Y. Chang, J. Carlson, V. R. Pandharipande, and K. E. Schmidt, Phys. Rev. A **70**, 043602 (2004); J. Carlson and S. Reddy, Phys. Rev. Lett. **95**, 060401 (2005).
[29] Y. Nishida and D. T. Son, Phys. Rev. Lett. **97**, 050403 (2006); G. Rupak, T. Schafer, and A. Kryjevski, Phys. Rev. A **75**, 023606 (2007).
[30] J. W. Chen and E. Nakano, Phys. Rev. A **75**, 043620 (2007).
[31] I. Giannakis, D. Hou, H. Ren, and D. Rischke, Phys. Rev. Lett. **93**, 232301 (2004).
[32] I. Giannakis and H. Ren, Phys. Lett. B **611**, 137 (2005); Nucl. Phys. **B723**, 255 (2005).
[33] K. Rajagopal and R. Sharma, Phys. Rev. D **74**, 094019 (2006).